

A hybrid geometallurgical study using coupled Historical Data (HD) and Deep Learning (DL) techniques on a copper ore mine

Alireza Gholami ¹, Kaveh Asgari ², Hamid Khoshdast ³, Ahmad Hassanzadeh ^{4,5}

¹ Department of Mineral Processing, Faculty of Engineering, Tarbiat Modares University, 14115111, Tehran, Iran

² FOCUS Minerals Engineering Research Center, Research and Development Division, Zarand, Iran

³ Department of Mining Engineering, Higher Education Complex of Zarand, 7761156391, Zarand, Iran

⁴ Department of Geoscience and Petroleum, Faculty of Engineering, Norwegian University of Science and Technology, 7031 Trondheim, Norway

⁵ Maelgwyn Mineral Services Ltd, Ty Maelgwyn, 1A Gower Road, Cathays, Cardiff CF24 4PA, United Kingdom

Corresponding author: ahmad.hassanzadeh@ntnu.no (Ahmad Hassanzadeh)

Abstract: This research work introduces a novel hybrid geometallurgical approach to develop a deep and comprehensive relationship between geological and mining characteristics with metallurgical parameters in a mineral processing plant. This technique involves statistically screening mineralogical and operational parameters using the Historical Data (HD) method. Further, it creates an intelligent bridge between effective parameters and metallurgical responses by the Deep Learning (DL) simulation method. In the HD method, the time and cost of common approaches in geometallurgical studies were minimized through the use of available archived data. Then, the generated DL-based predictive model was enabled to accurately forecast the process behavior in the mineral processing units. The efficiency of the proposed method for a copper ore sample was practically evaluated. For this purpose, six representative samples from different active mining zone were collected and used for flotation tests organized using a randomizing code. The experimental results were then statistically analyzed using HD method to assess the significance of mineralogical and operational parameters, including the proportions of effective minerals, particle size, collector and frother concentration, solid content and pH. Based on the HD analysis, the metallurgical responses including the copper grade and recovery, copper kinetics constant and iron grade in concentrate were modeled with an accuracy of about 90%. Next, the geometallurgical model of the process was developed using the long short-term memory neural network (LSTM) algorithm. The results showed that the studied metallurgical responses could be predicted with more than 95% accuracy. The results of this study showed that the hybrid geometallurgy approach can be used as a promising tool to achieve a reliable relationship between the mining and mineral processing sectors, and sustainable and predictable production.

Keywords: hybrid geometallurgy, historical data, deep learning, copper ore, flotation

1. Introduction

Today, due to the growing demand from many industries for various types of metallic and non-metallic minerals, researchers active in the field of geology and mining engineering, are always trying to improve methods of collaboration between the two sectors of mining and mineral processing (Lang et al., 2018). This relationship is important because changes in feed quality input to the mineral processing plant have always been a major challenge to achieving sustainable production. For this reason, accurate quantitative and qualitative knowledge of feed characteristics that are directly monitored and controlled by the geology and mining sectors is essential to achieve the short and long term goals over the lifespan of the mine (Parian et al., 2018a,b). On the other hand, by reducing the grade of mines and the complex textural characteristics of the extraction zones and as a result, the increasing variability of the feed of mineral processing units, achieving products with uniform quality

and quantitative characteristics may face with financial and technical problems (Yingling, 1990; Tungpalan et al., 2015). For this reason, traditional methods based on experience, qualitative observations and visual assessments will not be able to guarantee a sustainable process and must be supported by more accurate methods of characterizing mineral reserves (Pérez-Barnuevo et al., 2018).

An engineered approach to improve the productivity of traditional methods of characterizing mineral resources is defined in the form of geometallurgy. Geometallurgy is an interdisciplinary approach that provides the link between geological, especially mineralogical, and metallurgical information so that production engineers can plan and manage production much desirably (Parian et al., 2015). Geometallurgical studies are basically based on mineralogical information because the mining program is developed based on geological and mineralogical information so that the mine unit is able to deliver food with minimal mineralogical and grade changes to the mineral processing unit (Hoal, 2008). On the other hand, this information is the basis for evaluating and valuing ore deposits and designing beneficiation circuits by process development companies (Parian et al., 2015). Also, in recent years, with the development of instrumental characterization methods of minerals, the tendency to develop geometallurgical research has increased and several studies have been conducted in the field, such as base metals (Triffett et al., 2008; Alruiz et al., 2009; Lund et al., 2013; Amer et al., 2014; Navarra et al., 2017; Dehaine et al., 2021, 2022), platinum group metals (Becker et al., 2009), rare metals (Dehaine et al., 2019) and diamonds (Hoal et al., 2009), sand heavy minerals (Philander and Rozendaal 2013, 2014).

In general, geometallurgical studies include the development of maps of mineralogical changes in the ore deposit in order to predict the metallurgical efficiency of the mineral processing plant in a satisfactory way. Such connections are known as geometallurgical models and are a powerful tool in process improvement, production planning and technical decision making (Parian et al., 2015). Mineralogy-based geometallurgical modeling using information on the types of minerals present, their texture and chemical composition, as well as their mass proportions in the ore body, will be able to predict the metallurgical responses, usually concentrate grade, recovery and yield, for geological volumes or blocks, either individually or in blend, which have already prepared for mineral processing plant feed in different time periods and scales (Parian et al., 2018a; Pérez-Barnuevo et al., 2018). Despite the significant successes, the development of geometallurgical models faces several challenges. For example, geometallurgy requires extensive and expensive characterization studies to make the relationship between mineralogical block models and predict mineral processing behavior (Pérez-Barnuevo et al., 2018). On the other hand, each mining project will require a different geometallurgical model according to its specific geological characteristics, and therefore, it is not possible to develop a single, unique geometallurgical model for all mining projects, or at least the majority of them. The simplest approach in geometallurgical studies is to establish a relationship between the mineralogical characteristics of an ore body and the recovery of different minerals. However, in the mineral processing operation of a particular ore, several other parameters are also effective, such as the oversize and fines contents, mineral grade and heavy mineral composition, and physical/chemical properties of particle including size, shape, density, surface exposure, mineral liberation and particle chemistry (Philander and Rozendaal, 2014).

A review of geometallurgical studies shows that one of the most important aspects of the cross-linking process between mining and mineral processing is the interaction between operating factors such as solid percentage, the type and concentration of flotation reagents, and mineralogical parameters, that has generally been ignored. In addition, recovery is not the only metallurgical response in the evaluation of mineral processing processes, and other parameters such as the grade and tonnage of the concentrate and even the final moisture are also important. Parian et al. (2018a) divided geometallurgical studies into three levels based on the modeling objectives, i.e. the least detailed, moderate and the detailed levels, which according to the volume of information processed, predict the metallurgical behavior of the entire plant (whole processing circuit), sections of a single operation and single unit operations, respectively. However, the selection of any of the above levels also comes with limitations that make their usability a challenge. One of the most important of these restrictions rises when the geometallurgical model becomes unable to predict process behavior outside the range of data used to develop the initial model.

Despite the relatively simple mechanical and physical aspects, mineral processing processes have a very complicated mechanism. Such complexities mainly come from the multiplicity metallurgical and operational factors involved in the system as well as the interactions among them. Therefore, modelling and simulation of mineral processing processes have been always a challenging issue of debate. A recent approach to simulate complicated separation techniques is to use expert system methods (ESM) such as artificial neural networks, genetic algorithm etc (Asadi et al., 2020; Shamshirband et al., 2020; Apaydin et al., 2020). These intelligent algorithms transmit the knowledge or the rule behind data into a network structure by processing experimental data. ESM can be utilized to implement difficult functions in numerous areas, such as pattern recognition, visual system, classification, control, etc. Nowadays, problems that are difficult for human or ordinary computers can be solved by properly training intelligent algorithms (Hoseinian et al., 2020; Khoshdast et al., 2021; Gholami et al., 2021). One of the main applications of ESMs is forecasting based on a set of input data that has also yielded excellent results. Thanks to their good performance, ESMs have been frequently used in various scientific fields, including mining and mineral processing.

For example, Jorjani et al. (2008) simulated the rare earth elements leaching process of apatite concentrate using artificial neural networks (ANN) and showed that the process could be modeled using the improved ANN algorithm on an industrial scale with a reasonable accuracy. Later, Milivojevic et al. (2012) simulated the nickel ore leaching process to show that expert systems are more accurate than statistical modeling using linear regression. In another research work, Hoseinian et al. (2017) simulated copper recovery during a column leaching process of a copper ore sample on a pilot scale using a hybrid neural genetic algorithm and revealed that reliable prediction results could be obtained using an appropriate algorithm. Recently, Sobouti et al. (2019) modeled lead recovery during the lead concentrate leaching process using a combination of artificial neural network and particle swarm optimization (PSO) methods. The noteworthy point in this study was the large number of operational parameters including leaching time, liquid/solid ratio, stirring speed, temperature and fluoroboric acid concentration, that were used in the simulation process. They showed that using an optimized ANN-PSO algorithm, the process can be simulated effectively. The successful application of artificial neural networks in simulation of mineral processing operations has also been reported by Vyas et al. (2020). They showed that using ANN method, the spent catalyst bioleaching process can be simulated with acceptable accuracy and process responses can effectively be predicted. Ghobadi et al. (2011) applied genetic algorithm method to simultaneously model and optimize of a copper flotation circuit. They showed that using an oriented genetic algorithm can decrease the calculation time by 1/60 for a two-stage flotation system compared to conventional mathematical methods and provide higher optimization accuracy. In another study, Gholami and Khoshdast (2020) showed that using the ANN method, multiple metallurgical responses of the bioflotation process of a coal sample can accurately be simulated with a limited number of operating data. They evaluated different algorithms for the development of the ANN model and showed that the accuracy of the simulation results depends to a large extent on the correct choice of the network algorithm.

The most important point emerging from the above studies is that using intelligent modeling methods, mineral processing operations can be effectively simulated by considering the desired operational and process parameters and the limited number of data. Referring to the results reported in the above studies reveals that the accuracy of the simulation in most cases has been more than 95%, which is very desirable in terms of application. Therefore, given that geometallurgical studies often require large volumes of data, the use of intelligent approaches can help reduce execution time, and sampling and characterization costs. Thus, the aim of this research is to introduce the concept of "hybrid geometallurgy" by coupling the statistical method of Historical Data (HD) and intelligent technique of Deep Learning (DL) as a novel and efficient geometallurgical approach to reduce the number of test works, to involve more applied parameters in the geometallurgical model development process and to consider the interactions between mineralogical and metallurgical parameters. The effectiveness of this new approach for a copper mine was successfully evaluated. To the best of the authors' knowledge, this is the first reported case in the field of geometallurgy.

2. Materials and methods

2.1. Sampling and sample characterization

Since the main objective of this study is to investigate the variation in the metallurgical behaviour of the processing plant in response to the mineralogical changes of input feed, six zones of the active mining areas were selected and sampled based on the opinion of the company supervisors. The geographical coordinates and characteristics of the sampled zones are presented in Table 1.

Initially, 200 kg of the ore was sampled from each mining face using automatic sampling machines. The sample was immediately transferred to the laboratory for crushing and preparation operations to prepare representative samples for the mineralogical assessments. All assaying, mineralogical analyses and determination of liberation degrees were performed in Miduk Copper Complex laboratories based on standard methods of optical, X-ray diffraction (XRD) and X-ray fluorescence (XRF) microscopic analyses.

Table 1. The geological and geographical properties of the sampling points

Sample no.	Bench no.	Blast no.	Geological type	GPS coordinations			Representative minerals	Representative gangues
				X	Y	Z		
1	2570	649	Supergene/Phyllic/Argillic alteration	2570	6635.63	4184.79	Chalcocite	Pyrite, Sericite
2	2450	169	Supergene/Phyllic alteration	2450	7395.35	4027.05	Chalcocite	Pyrite
3	2420	62	Hypogene/Potassic	2420	7161.67	3924.24	Chalcopyrite	Pyrite
4	2480	236	Supergene/Phyllic/Argillic alteration	2480	7452.72	3728.45	Chalcocite	Pyrite, Sericite
5	2420	64	Hypogene/Potassic/Phyllic	2420	7287.88	3957.2	Chalcopyrite, Bornite	Pyrite
6	2420	48	Hypogene/Potassic/Phyllic	2420	7043.88	3845.6	Chalcopyrite	Pyrite

2.2. Experimental variables and historical data (HD) design

To select the effective parameters and their levels, the operating conditions of the concentration plant were monitored and analyzed throughout the last five years (from 2016 to 2021). As a result, based on changes in the qualitative and quantitative conditions of the final concentrate as well as the expectations of plant's authorities, five operating factors including flotation feed size, collector and frother concentrations, solid content and pH of the input pulp to the flotation circuit were selected. The upper, middle and lower levels of these variables are presented in Table 2. It should be noted that these levels have been selected based on the monitoring results. To investigate the effect of ore mineralogy on the efficiency of flotation process, the amount of all copper-bearing minerals, sphalerite, pyrite and other iron-associated minerals is presented in Table 2.

Since one of the main purposes of this study was to simulate the geometallurgical correlations with process variables using expert systems, the number and conditions of experiments were determined in a way that there is no regular relationship among them. For this purpose, a specified code in Matlab software (MathWorks R2021b v9.11, Natick, MA, USA) was developed to adjust the test conditions to: a) each variable must appear at least once in the experimental design, b) each level of each variable must appear at least once in the experimental design, c) the experiments are randomly sorted in the final experimental design, d) each experiment should not be replicated more than twice, and e) replications should not include more than half of the total of the main experiments. The last two steps were defined in order to determine the error of statistical analysis and to prevent overlap (bias) of the main effects of the variables with each other (Khoshdast et al., 2021). Finally, 66 individual experiments were designed, and performed according to the experimental design created by the developed code.

Since the experiments suggested by the developed MATLAB code were statistically unordered, statistical analysis and evaluation of the significance of various operational and mineralogical varia-

Table 2. Types and levels for various operating and mineralogical variables

Operating variables					
Level	Particle size (d_{80} , μm)	Collector conc. (C , g/t)	Frother conc. (F , g/t)	Solid content (X , w/w%)	pH
Low	63	32	10	25	11
Mid	90	37	13	30	11.5
High	110	40	16	35	12
Mineralogical variables					
Level	Chalcocite (C_c , %)	Covellite (C_v , %)	Chalcopyrite (C_p , %)	Sphalerite (S_p , %)	
Low	0.02	0.00	0.06	0.11	
High	0.33	0.08	2.45	0.27	
Level	Pyrite (P_y , %)	Hematite (H_m , %)	Magnetite (M_g , %)	Limonite (L_m , %)	
Low	5.33	0.00	0.00	0.00	
High	17.2	0.21	0.29	0.56	

bles was conducted using historical data (HD) method. The HD method is a new approach in the design and analysis of experiments. Unlike conventional designs such as full factorial and response surface, which lack a pre-designed structure based on statistical principles, HD design allows the engineers to evaluate the significance of the desired parameters with any number of levels. This very useful feature is extremely beneficial for statistical analyses of industrial data recorded over time or in industrial studies where it is impossible to use conventional experimental designs due to uncontrollable fluctuations. It should be noted that in the HD method, if the number of process variables is large, it is not possible to examine the interactions between the variables due to the bias (Montgomery, 2001). However, in this method, like other conventional designs with a regular and predefined structure, data analysis was performed by developing statistical models, analysis of variance (ANOVA) and using the main effect plots. Therefore, due to the nature of geometallurgical studies based on the analysis of large volumes of mineralogical and metallurgical data recorded over a long time, the use of HD method is a practical and reliable approach that is proven for data studied in this research work.

2.3. Flotation experiments and calculations

All the flotation experiments were carried out in a standard Denver D-12 flotation machine equipped with a 2 L cell. The pulp level was maintained constant by continuously adding water as required. For each experiment, an appropriate amount of the ore sample was mixed with 1 L of tap water to reach a desirable solid content. It was then agitated at an impeller speed of 1000 rpm for 5 min in the flotation cell to ensure that all ore particles were well suspended. Following conditioning, the cell was filled with water to a set level. Then, combination of collectors with the mixture of Z-11 (sodium isobutyl xanthates), X231 (O-isopropyl-N-ethyl thionocarbamate) and A3477 (sodium diisobutyl dithiophosphate) was added and conditioned for 3 min. After conditioning, the requisite amount of frother as a mixture of A65 (a polyglycol ether with molecular weight of 395.61) and MIBC (methyl isobutyl carbinol) was added and conditioned for another 2 min. Flotation was continued for 12 min until the froth zone was weighed. All experiments were conducted in kinetic mode by collecting concentrated froths during predetermined sampling intervals. At the end of each experiment, the collected concentrates and tailings were weighed and dried in an oven at 60°C over night (Khoshdast et al., 2012).

The efficiency of the flotation process was evaluated in terms of final recovery and grade of Cu and Fe using the following Equation (Khoshdast et al., 2011):

$$R = \frac{C}{F} \times \frac{c}{f} \times 100 \quad (1)$$

where R (%) is recovery, F and C are the total mass of feed and concentrate, respectively, f (%) and c (%) are element grade (%) of feed and concentrate, respectively. To investigate the effect of variables

on the flotation rate of copper, the kinetic constant of the flotation process was calculated using the classical first-order kinetics equation (Gholami and Khoshdast, 2020):

$$R = R_{\infty}(1 - e^{-kt}) \quad (2)$$

where R_{∞} (%) is the maximum achievable recovery, k (1/min) is the flotation rate constant and t (min) is the flotation time.

2.4. Deep learning simulation

2.4.1. Preliminary data studies and normalization

In this study, 10 inputs were included as particle size (μm), collector concentration (g/t), frother concentration (g/t), solid content (w/w%), pH (as the operating conditions), chalcocite (%), covellite (%), chalcopyrite (%), pyrite (%) and sphalerite (%) (as the mineralogical data). The outputs were Cu grade (%), Cu recovery (%), Fe grade (%) and Cu kinetics rate (1/min) that four models were developed to predict them based on the inputs. The statistical summary of the data is presented in Table A1.

Data distribution was also examined to understand normal or non-normal distribution of the data. Kolmogorov-Smirnov test of normality was chosen because it does not need the underlying population distribution of the data to run it and has no restrictions on sample size. K-S test was applied to the data using IBM SPSS Statistics version 26 software. A 95 percent confidence interval was used for the K-S test and the software null hypothesis was that the data are not normally distributed. After the K-S test, as shown in Table A2, p -values of all variables except the Cu kinetics rate are less than 0.05. Therefore, the null hypothesis is confirmed and the data is not normally distributed. Besides, normalization was applied by re-scaling all data to a standard frame to boost the network training phase. The inputs and the outputs are normalized using Equation (3) to rescale them in the range of [-1,1]:

$$X_n = \left(\frac{X_i - X_{min}}{X_{max} - X_{min}} \right) \times 2 - 1 \quad (3)$$

where X_n and X_i are normalized and actual values, respectively. X_{min} and X_{max} are the minimum and maximum values of each subset (inputs–outputs).

2.4.2. Long short-term memory neural network (LSTM)

Recurrent Neural Networks (RNNs) are the most widely used deep learning techniques for predicting time series data. Unlike the traditional neural networks, RNNs are able to store past information in the network and use it to process a sequence of inputs. But the main issue of RNNs is vanishing gradient and exploding gradient problems as described by Bengio et al. (1994). Gradient descent optimization algorithm is used to train RNNs. In this optimization algorithm, each parameter changes according to its effect on the final result of the network. This is implemented by a partial derivative of the error function for each parameter in each iteration of the training process. The vanishing problem refers to the fact that the values of the gradients gradually become so small that the training process is severely slowed down or stopped. Long short-term memory neural network (LSTM) is developed to cope the challenge of vanishing gradient problem (Calin, 2020). LSTM is a special kind of RNN which was first introduced by Hochreiter and Schmidhuber (1997). They are capable of learning long-term dependencies and remembering information for long time periods (Le et al., 2019). This deep neural network can be used for both classification and estimation purposes.

In this study, to estimate the outputs, LSTM was used to develop four models based on input data. There are new concepts in LSTM neural networks that did not exist in traditional RNNs. In this network, there are three gates through which the network controls the data flow inside including forget gate, input gate, and output gate. In addition to these three gates, the main component of this type of network is the cell state, so-called long-term memory. The cell state connects all LSTM blocks and allows information to be added to or removed from the network (Graves, 2012). Also, all recurrent neural networks are in the form of repetitive sequences of neural network blocks. These

repetitive blocks are shown in Fig. 1(a). For more information on the LSTM neural networks, more detailed information can be found elsewhere (Bernico, 2018).

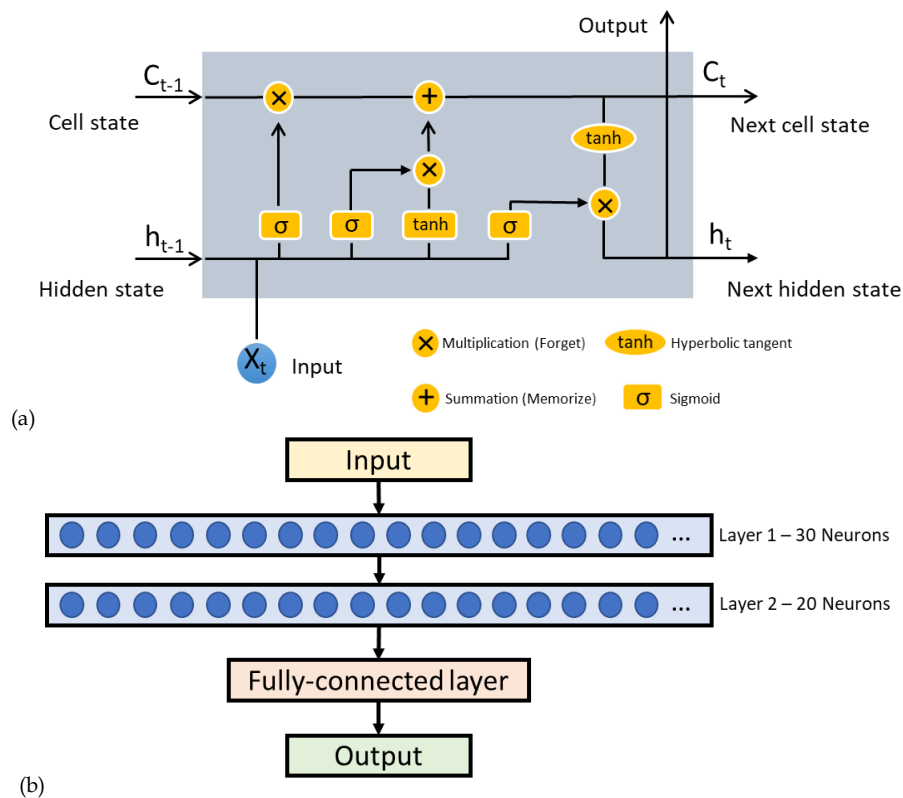


Fig. 1. The structure (a) and proposed architecture (b) of long short-term memory neural network

2.4.3. LSTM neural network design

MATLAB software was used to develop codes, LSTM networks and to perform the modeling process. The number of neurons in the input and output layers depends on the number of inputs and outputs of the problem. In this study, number of input and output layers of neurons is ten and one, respectively. The number of hidden layers is directly related to the complexity of the problem, and in most problems with different complexities, two or at most three hidden layers were sufficient. Also, implementing more than three hidden layers was non-optimal in terms of time complexity (Uzair and Jamil, 2020). Our models are comprised of two LSTM layers with 30 and 20 neurons, followed by a fully connected layer for generating outputs. The fully connected layer causes the network result to be presented in the form of a vector with a specified size. Fig. 1(b) depicts the architecture of the proposed LSTM network.

To train models, batch size was set as 10, meaning that parameters were updated every 10 training samples. Max Epochs which defines the number of times that the learning algorithm work through the entire training dataset was adjusted at 40. Adam algorithm was used to optimize the weights in each level. In addition to speed, this algorithm is highly efficient on systems with low memory. Other parameters including Gradient Threshold, Initial Learn Rate, Learn Rate Drop Period and Learn Rate Drop Factor were also adjusted as shown in Table A3. The data was also divided into training (70 %), testing (20 %) and validation (10 %) matrices in a way that validation data increased the quality of the training process and prevented over-fitting.

3. Results and discussions

3.1. Elemental and mineralogical studies

The results of mineralogical analyses of the studied samples are presented in Table 3. The chalcopyrite content of sample 5 is 2.45%, while samples 3 and 6 have the highest amount of chalcopyrite. Samples

4, 1 and 2 contain small amounts of chalcopyrite. In samples 2 and 4, the amount of covellite is 3 times more than samples 5 and 6, and sample 3 has the lowest amount of covellite among the samples. Samples 1 and 3 have higher chalcocite than other samples, but these two minerals are not liberated well in these respective ores; this is while samples 5 and 6 with the amounts of 0.045 and 0.021% have the lowest amount of chalcocite, the same small amount of which are completely liberated. Sample 2 has the highest amount of sphalerite and samples 5 and 4 contain small amounts of this mineral. Samples 1, 3 and 6 also have the same amount of sphalerite. Samples 2 and 1 contain the highest amount of pyrite, respectively, while the proportion of pyrite in the other samples is almost the same. Sample 5 has the highest amount of hematite compared to other samples. Sample 2 also lacks the hematite mineral. Samples 4 and 6 have the highest amount of magnetite and samples 1 and 2 do not have this mineral. Samples 1 and 2 have no limonite mineral, while sample 5 with 0.558% has the highest amount of limonite.

The results of chemical analysis of the samples are presented in Table 4. According to the results, sample 5 with a grade of 0.95% has the highest grade of copper, and samples 2 and 4 with a value of 0.21 and 0.18, respectively, have the lowest amount of copper.

Table 3. Percentage of key minerals considered in metallurgical studies for different samples

Sample no.	Chalcocite	Covellite	Chalcopyrite	Sphalerite	Pyrite	Hematite	Magnetite	Limonite
1	0.330	0.030	0.107	0.164	12.442	0.119	0.000	0.000
2	0.087	0.076	0.115	0.274	17.196	0.000	0.000	0.000
3	0.106	0.004	1.248	0.165	5.334	0.131	0.148	0.065
4	0.099	0.077	0.058	0.109	5.464	0.145	0.251	0.025
5	0.045	0.021	2.454	0.122	5.721	0.210	0.114	0.558
6	0.021	0.018	1.275	0.171	6.603	0.199	0.295	0.148

Table 4. Percentage of key elements considered in metallurgical studies for different samples

Sample no.	1	2	3	4	5	6
Cu	0.390	0.210	0.540	0.180	0.950	0.490
Fe	5.920	8.060	3.580	3.340	4.000	3.920

3.2. Development of historical data model

The first step in analyzing the impact of operational variables on process responses in order to develop a parametric model that can accurately predict the desired response in the operating space, i.e. within the low to high levels intended for variables (Boveiri et al., 2019). In this study, Design Expert v.7.0 software was used to model experimental data. An essential feature of the HD approach is that, unlike other standard designs, it is possible to fit more models to experimental data. In the second step, after the development of the initial model by the software, abnormal data were identified by examining the model parameters and the model was optimized by the user to achieve the best fitting results. The result of these measures for the data obtained in flotation experiments was the development of Response Surface Reduced Linear model for all process responses as below:

$$Cu \text{ Grade } (\%) = -22.27 - 0.04 \times d_{80} - 0.25 \times C - 0.16 \times F - 0.23 \times X + 1.32 \times pH + 83.78 \times Cc + 182.90 \times Co + 11.50 \times Cp - 3.41 \times Py + 244.37 \times Sp \quad (4)$$

$$Cu \text{ Recovery } (\%) = 0.07 \times d_{80} + 1.10 \times C + 3.31 \times F + 1.49 \times X - 2.31 \times pH - 193.99 \times Cc - 261.17 \times Co + 2.55 \times Cp + 4.28 \times Py - 264.43 \times Sp \quad (5)$$

$$Fe \text{ Grade } (\%) = 0.08 \times d_{80} + 0.27 \times C - 0.05 \times F - 0.18 \times X - 4.39 \times pH + 85.78 \times Cc + 359.77 \times Co + 11.47 \times Cp - 2.46 \times Py + 275.02 \times Sp \quad (6)$$

Rate Constant (1/min)

$$= 0.01 \times d_{80} + 0.02 \times C - 0.09 \times F - 0.02 \times X + 0.25 \times pH - 6.55 \times Cc - 20.49 \times Co - 0.14 \times Cp + 0.11 \times Py - 4.31 \times Sp \quad (7)$$

where d_{80} , C , F , X and pH are operational parameters respectively including particle size (μm), Collector concentration (g/t), Frother concentration (g/t), Solid content (%w/w) and pulp pH, and Cc , Co , Cp , Py and Sp correspond to mineralogical contents (%) of chalcocite, covellite, chalcopyrite, pyrite and sphalerite, respectively.

The validation parameters for the developed models are listed in Table 5. As shown in Table 5, the suggested prediction models are all significant due to their high value of Fisher's F-test (almost > 30) and marginal probability value (p model < 0.0001). The residuals normal probability plot is an efficient tool for evaluating the significance of the prediction model (Yetilmezsoy et al, 2009). The relatively uniform normal probability plots for all responses are shown in Fig. 2 confirming the normality assumptions and independence of the residuals during the statistical analyses. In addition, the high values of the adjusted correlation coefficients ($\text{Adj } R^2 > 85\%$) also indicate significance of the prediction models. The $\text{Pred } R^2$ values were also reasonably high, implying that the model can explain variability in predicting new observations with acceptable accuracy, which is in reasonable agreement with the $\text{Adj } R^2$ values (Shak and Wu, 2015). Adeq precision is also another statistical measure showing the signal to noise ratio; the desirable value is greater than 4 (Montgomery, 2001). In this investigation, the ratios were 21.07, 11.03, 8.98 and 10.71 for copper grade and recovery, iron grade and kinetic rate, respectively. These values imply an adequate signal so that the models can be used to navigate and predict the design space.

Table 5. Validation measures of models developed for process responses

Measure	Cu grade (%)	Cu recovery (%)	Fe grade (%)	Rate constant (1/min)
F value	62.9624	79.7547	39.8100	40.0570
p -value	< 0.0001	< 0.0001	< 0.0001	< 0.0001
Std. Dev.	2.0641	19.9131	7.6594	0.5851
R-squared	0.9251	0.9421	0.8825	0.8831
Adj R-squared	0.9104	0.9303	0.8603	0.8611
Pred R-squared	0.8875	0.9180	0.8376	0.8373
Adeq precision	21.0733	11.0301	8.9823	10.7135

3.3. Statistical analysis of main effects

Model equations 4-7 were used to assess the significance of operating variables on process responses. Tables A4 to A7 show the ANOVA results within a confidence interval of 95%. As shown in Tables A4-7, the effects of all operational variables on process responses are statistically meaningful due to p -values less than 0.05. It is also noteworthy that the effects of mineralogical factors are more significant than metallurgical factors (p -value < 0.0001). As can be seen in the analysis of variance tables, no interaction was considered in the analyses. In HD studies, due to the lack of repetition, different interactions will overlap, and therefore, their analysis is not possible independently. On the other hand, due to the resultant bias, the development of the models has been done using only the main effects. However, studies have shown that considering the interactions, the accuracy of the model either did not change much or even decreased in some cases. The main effects plots of different operating variables are shown in Figs. 3 to 12 for different responses. These plots are an effective tool for evaluating the influence of each variable on the target response.

3.4. Interpretation of the effects of operating variables

The role of operating parameters in the grade and recovery of copper and iron as well as copper flotation rate is shown in Figs. 3 to 7. As can be seen, with increasing particle size and thus decreasing the degree of freedom, the grade and recovery decreases. This effect can be clearly seen in the increase

in iron content in the concentrate by increasing the particle size. However, maximum recovery is achieved with a characteristic size of 90 μm which is optimal for this type of ores as shown in previous studies (Hassanzadeh and Karakas, 2017a, b). As the particle size decreases below 63 μm , although it improves through an increase in the degree of freedom, the recovery decreases because of production of a high amount of slimes and the increase of the entrainment rate. Significant reduction of copper recovery for fine fraction sizes have been addressed broadly in the literature and related fundamental and practical reasons can be found elsewhere (Hassanzadeh et al., 2018; Farrokhpay et al., 2021). Regardless of the nonlinear effect of the collector concentration, its impact on the grade and recovery is opposite to each other. Obviously, as the collector concentration increases and the particle hydrophobicity improves, the rate at which the gangue particles direct to the concentrate also increases and, as a result, the grade decreases. Although the effect of collector concentration on iron grade is not significant, but at medium concentration, iron grade in concentrate is maximized. This effect can be attributed to the fact that since the collector used in this study is actually a combination of three different collectors, at a certain concentration, the competitive action of these collectors has likely improved the hydrophobicity of iron minerals. In this regard, Agheli et al. (2018) investigated the effect of pyrite content of feed and configuration of locked particles on rougher flotation of copper in low and high pyritic ore types. They concluded that pyrite can be transferred to the concentrate through different physical and chemical mechanisms, which can be intensified for high-pyritic copper ores.

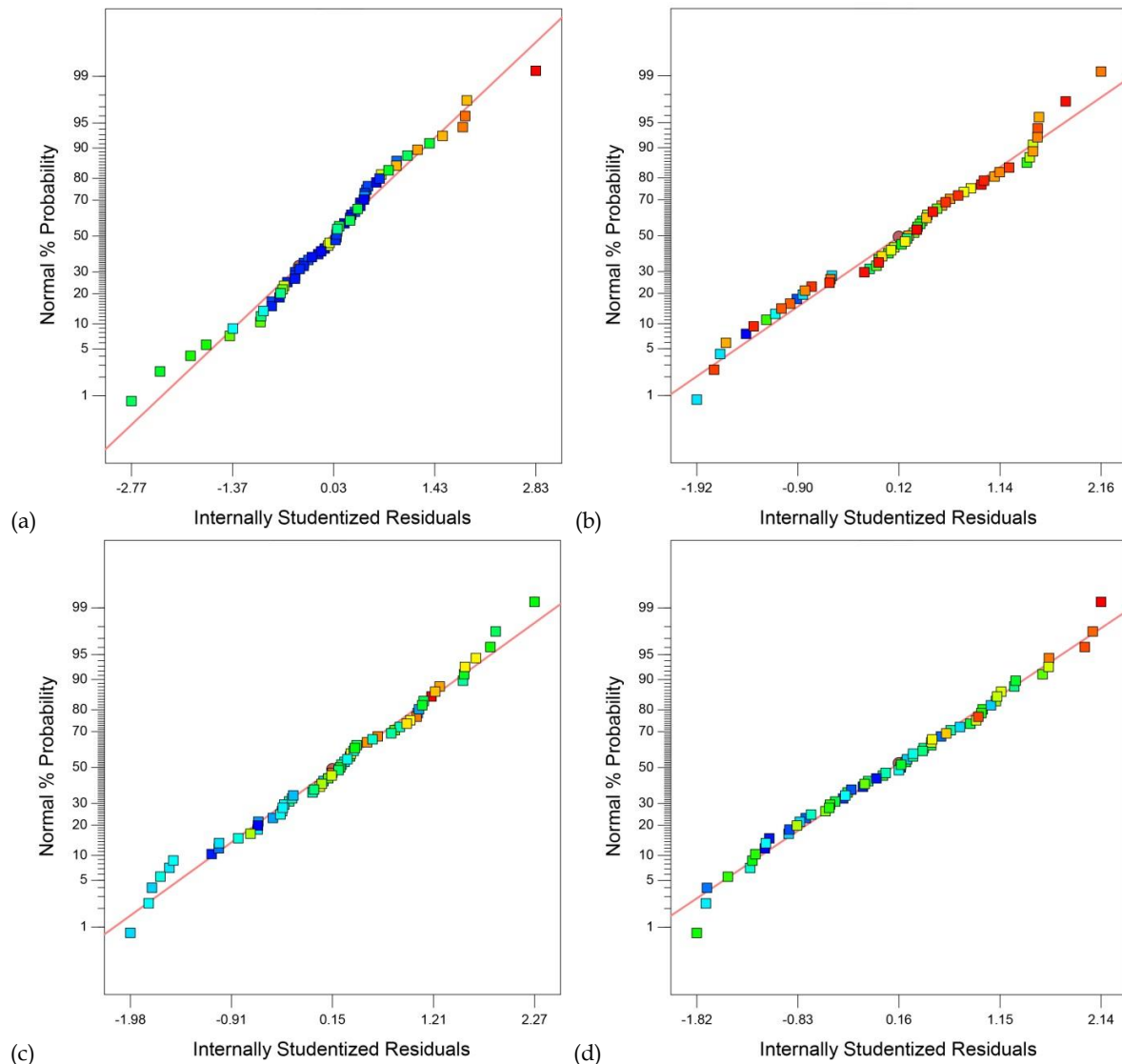


Fig. 2. Normal plot of the residuals for (a) Cu grade, (b) Cu recovery, (c) Fe grade, and (d) flotation rate constant

The effect of increasing the frother concentration on the copper grade is small but descending; however at the high level of this variable, the recovery has increased significantly. In general, recovery improves with rising frother concentration due to improved froth stability and reduced coalescence rate and consequent drop-back of particles to the pulp. The effect of froth stability in mechanical cells on the concentration of concentrate is very limited due to the low height of the froth phase and the descending trend observed in Fig. 5 can be attributed to the increased recovery of gangue particles to the concentrate. The decrease in iron content by changing the concentration of the frother can also be attributed to the phenomenon that with increasing the dosage of the frother, the size of the bubbles decreases and their ability to float iron-containing particles with higher density decreases.

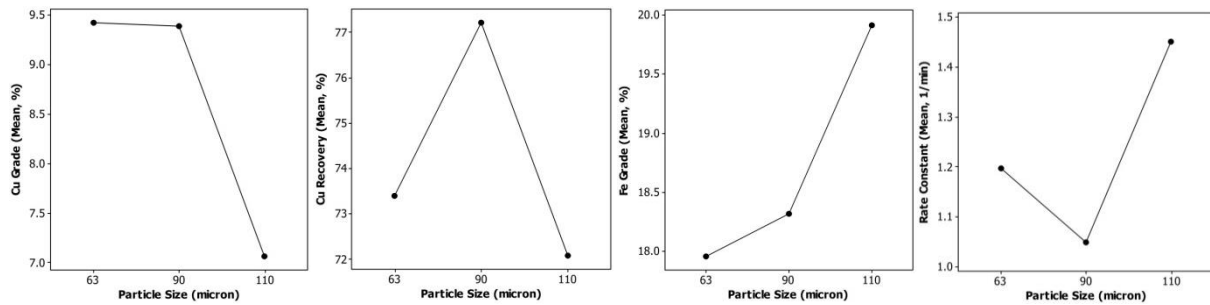


Fig. 3. Main effect plots showing the effect of particle size on metallurgical response

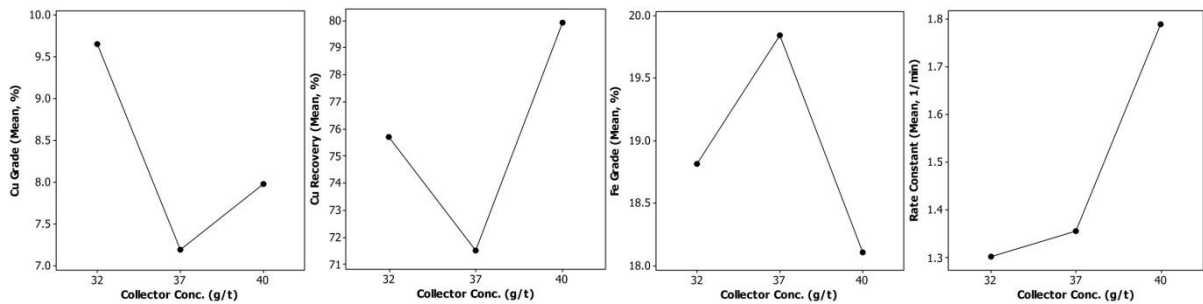


Fig. 4. Main effect plots showing the effect of collector concentration on metallurgical response

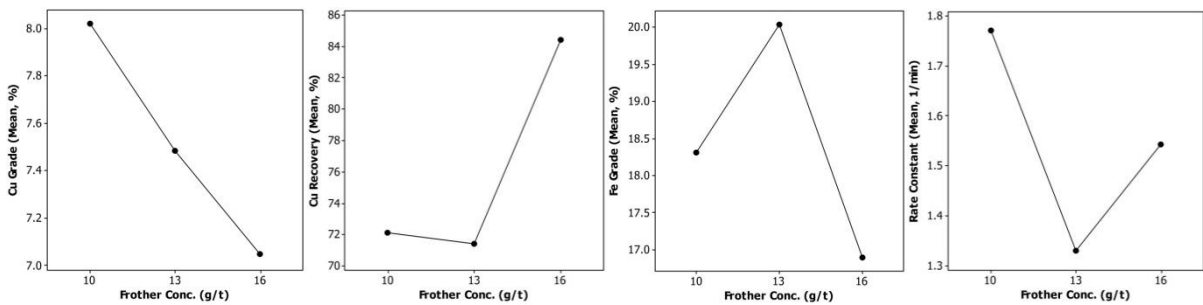


Fig. 5. Main effect plots showing the effect of frother concentration on metallurgical response

The effect of solid percentage on copper recovery is ascending and on iron grade is decreasing, while the maximum grade of copper is obtained in the middle level of this parameter. As the percentage of solid enhances, the rate of mechanical entrainment exceeds regarding the increase in the rate of turbulence in the pulp environment, resulting in improved copper recovery but a decrease in grade. As commonly known, there is an optimal range of solid content for each specific process to maximize the target mineral's ultimate recovery and kinetics rate. Azizi et al. (2015) reported that enhancing %S from 15% to 25% improved copper recovery but significantly attenuated by a further increase to 35%, which is in line with our observation. The pH of the pulp has a similar effect either copper grade or recovery, and the maximum of both metallurgical responses is obtained at the intermediate level, i.e., 11.5. Obviously, copper ore flotation is significantly dependent on pulp

chemistry and the best performance of flotation reagents for interaction with mineral surface occurs under optimal chemical conditions. The decrease in iron content in the concentrate with increasing pH can be attributed to the increase in pyrite depression rate by increasing the amount of lime, as a pH regulator and depressant of this mineral.

As can be seen in the results (Figs. 3-7), except for pH, the effect of other variables is nonlinear. As the particle size increases, the flotation rate decreases due to the reduced carrying capacity of bubbles, but as can be seen, the flotation rate increases again with increasing particle size. However, in these particle sizes, the grade and recovery of copper have decreased. This unusual behavior may be due to the interaction between some variables. Given that it is not possible to accurately assess the interaction between variables in HD studies, it is difficult to provide a definitive reason for this behavior. Hassanzadeh et al. (2019) addressed the impact of such interactive effects and reported contradictory results in the literature. As the collector concentration increases, the flotation rate increases due to improved particle hydrophobicity. In general, it is expected that the flotation rate increases with increasing frother concentration due to the improvement of bubble dynamic properties in the pulp phase, but according to Fig. 5, the flotation rate decreases with excessive frother concentration to the middle level first and then increases again. This behavior may be due to the interaction between frothers and collectors.

As with the frother concentration, the flotation rate is minimized at the intermediate level of the solid percentage and then increased. At low solid percentages, due to the steady conditions in the pulp environment, the particles are less likely to be released from air bubbles and therefore the flotation rate is improved. As the percentage of solid increases and as a result, the turbulence in the pulp increases, the bubbles release their loads and the flotation rate decreases. As the solid percentage increases and the hindered settling conditions prevail, the untrue flotation rate of the particles and, consequently, the total flotation rate increases again. The effect of pH on the flotation rate is linearly steep. Increasing the pH due to the increase in pyrite depression rate causes more copper mineral particles to float and consequently the copper flotation rate also increases.

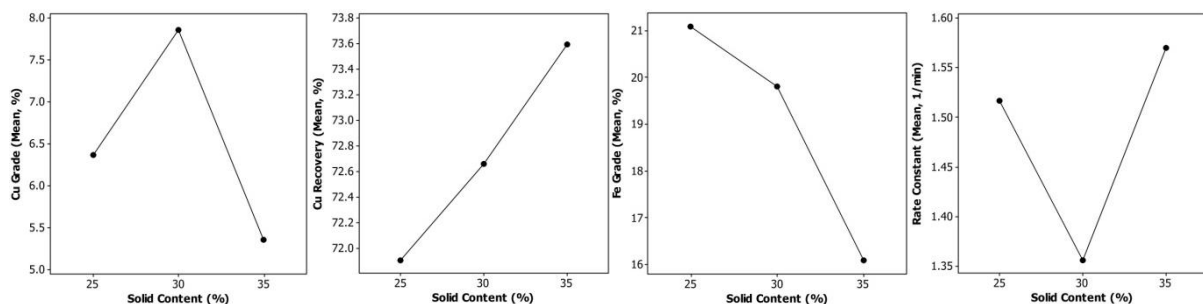


Fig. 6. Main effect plots showing the effect of solid content on metallurgical response

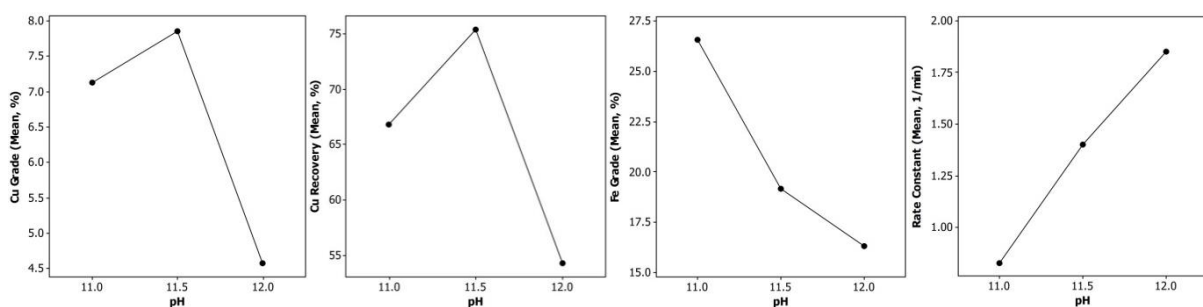


Fig. 7. Main effect plots showing the effect of pulp pH on metallurgical response

3.5. Interpretation of the effects of mineralogical variables

The effect of mineralogical characteristics on copper flotation performance is shown in Figs. 8-12. As can be seen, ore mineralogy has a very complex effect on the behavior of metallurgical responses, and this clearly confirms the need for geometallurgical studies. The fluctuations observed in all diagrams

are contributed to differences in the liberation degree of minerals in the sample studied. Table 6 shows the degree of freedom for target minerals in the samples. To ease analyzing the mineralogical composition effect on the behavior of the flotation process, the average trend diagrams of each response are also drawn.

According to the given results (Figs. 8-12), with increasing proportion of chalcocite (Cu_2S), the copper grade in the concentrate follows a decreasing trend, while with increasing the amount of chalcopyrite (CuFeS_2), the grade increases almost linearly. Although both minerals are sulfide and the collectors used in the process are suitable for the flotation of this type of minerals, the behavior of these two minerals in the flotation process is opposite to each other. According to Table 6, it can be seen that a higher degree of freedom does not necessarily improve the grade. For example, the liberation degree of chalcocite for samples with a grade of 0.099 (0.10 in the figure) and 0.106 (0.11 in the figure) is 100% and 50%, respectively, while the grade of concentrate for the case with lower liberation degree is far greater. The ratio of chalcocite to chalcopyrite (Cc/Cp) is also presented in Table 6. By comparing this ratio for the above two samples, it clearly shows that this ratio is vital to analyze the significant difference in behavior of these two samples. As can be seen in the table, the Cc/Cp ratio for the sample with the grade of 0.099% is equal to 1.7 and for the sample with the grade of 0.106% is equal to 0.09. Comparison of this ratio for other samples in the table indicates that the grade in concentrate improves by reducing this ratio. The reason for this can be attributed to the competition of chalcocite and chalcopyrite minerals in interaction with collectors. As the portion of chalcocite decreases, the portion of floated chalcopyrite increases. This effect is also clearly observed in the copper recovery behavior (Fig. 6). However, as the portion of chalcopyrite increases due to the higher iron content, the iron content of the concentrate also increases (Fig. 10).

Table 6. The percentage of liberation degree of minerals with significant effect

Sample no.	Chalcocite (%)	Chalcopyrite (%)	Cc/Cp	Covellite (%)	Pyrite (%)
1	51.35	6.25	3.06	0	80.24
2	90.48	100	0.76	63.54	98.61
3	50	94.25	0.09	100	98.01
4	100	77.27	1.7	100	96.09
5	100	98.15	0.02	80	89.39
6	100	100	0.02	100	100

Unlike high-grade copper ores, both the grade and recovery of copper decreases with increasing covellite (CuS) portion. According to Table 6, there is an inverse relationship between the grade and liberation degree of this mineral in the samples. The effect of increasing the grade of covellite on the grade of iron in concentrate is a decreasing trend, but at the highest grade of covellite, the grade of iron suddenly increases. Referring to Table 6, it can be seen that the degree of freedom of covellite in the sample with a high grade of this mineral is much lower than other samples (63.54%), and therefore, iron directly transfers to the concentrate with particles locked with covellite. According to Figs. 8 to 12, the copper grade has decreased sharply with increasing pyrite while the iron grade has increased significantly. Obviously, with increasing pyrite due to competition with flotation of copper minerals, copper recovery also decreases.

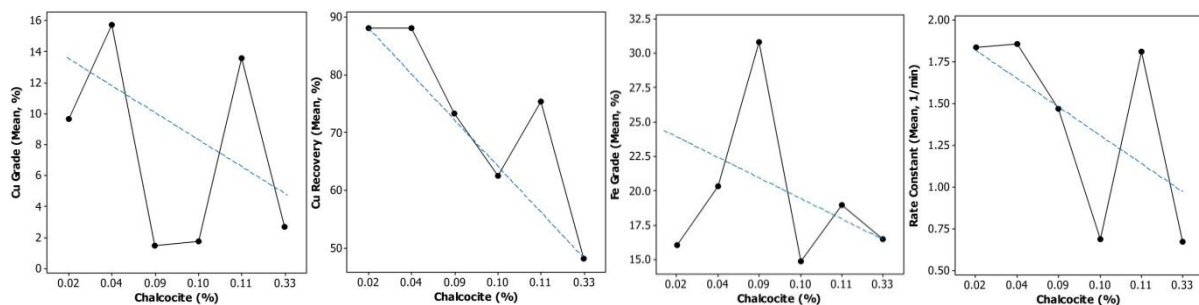


Fig. 8. Main effect plots showing the effect of chalcocite content on metallurgical response

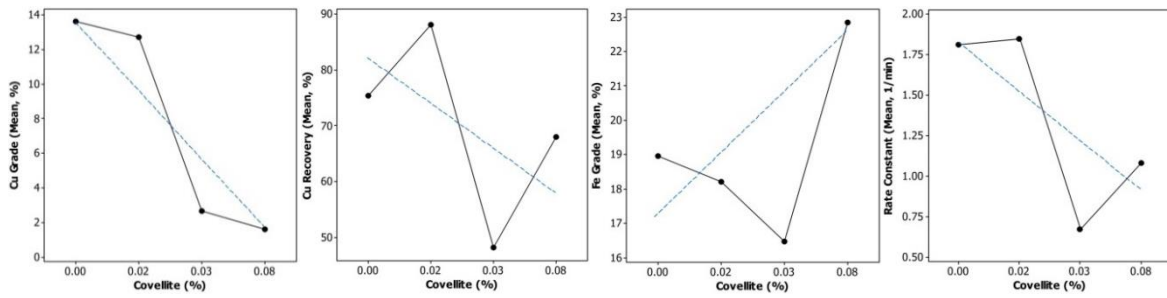


Fig. 9. Main effect plots showing the effect of covellite content on metallurgical response

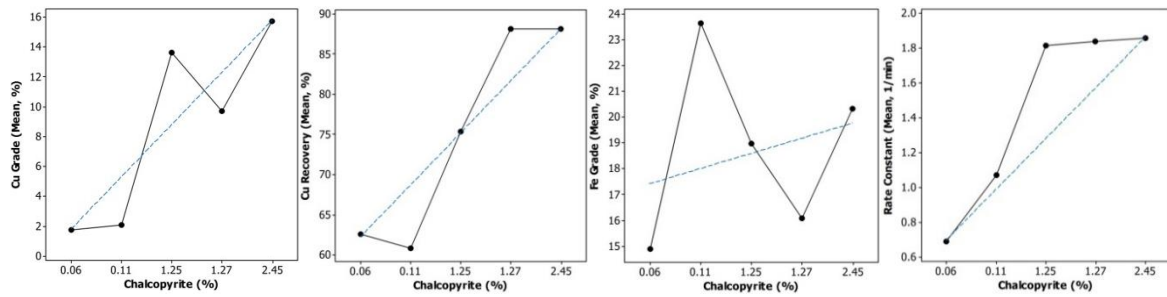


Fig. 10. Main effect plots showing the effect of chalcopyrite content on metallurgical response

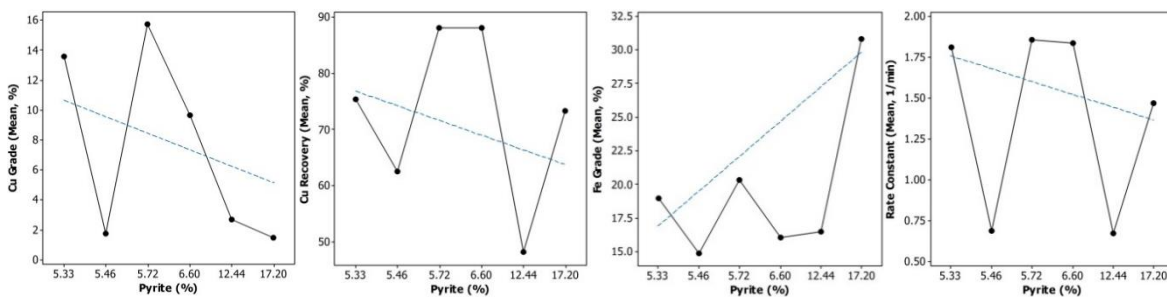


Fig. 11. Main effect plots showing the effect of pyrite content on metallurgical response

Another mineralogical parameter with a meaningful and significant effect on process responses was the sphalerite grade in the samples. In general, increasing sphalerite means boosting the rate of collector adsorption and competitive flotation with copper minerals and decreasing copper grade. The slight increase in copper recovery is also due to locking with other minerals and thus increasing the iron content in the concentrate. As can be seen, the trend of flotation rate changes is the same as the way copper recovery is influenced by the mineralogical properties of the input feed, and therefore, the same argument can be made for the trends observed in flotation rate plots.

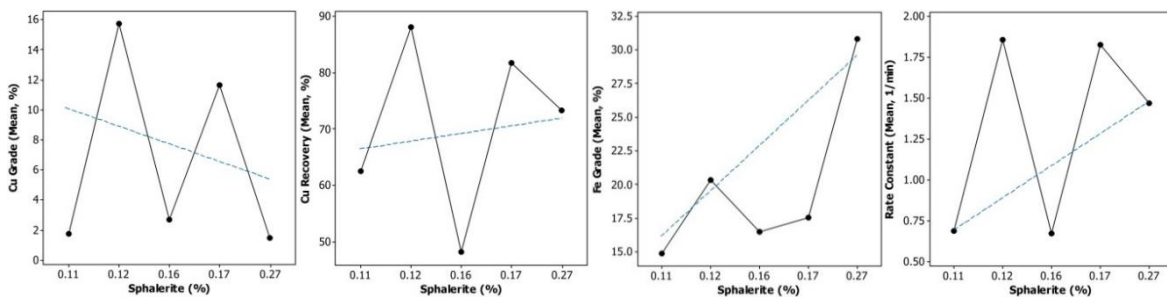


Fig. 12. Main effect plots showing the effect of sphalerite content on metallurgical response

3.6. Deep learning simulation results

To evaluate the network's performance, the mean squared error (MSE), root mean square error (RMSE), and percentage error were used. The following equations were applied to calculate the

respective errors and the estimation results in the form of accuracy. The results are listed in Table 7 for Cu grade, Cu recovery, Cu kinetics rate and Fe grade (Schober et al., 2018):

$$MSE = \frac{1}{n} \sum_{i=1}^n (y_i - y'_i)^2 \quad (10)$$

$$RMSE = \sqrt{\frac{1}{n} \sum_{i=1}^n (y_i - y'_i)^2} \quad (11)$$

Table 7. Estimated results for the outputs using LSTM networks

Algorithm	Training			Test		
LSTM for	MSE	RMSE	% Error	MSE	RMSE	% Error
Cu grade	2.3482e-06	0.001	0.077	0.007	0.086	4.302
Cu recovery	1.1672e-07	3.4165e-04	0.017	0.009	0.095	4.740
Cu kinetics rate	3.1371e-07	5.6010e-04	0.028	0.008	0.089	4.438
Fe grade	3.5781e-07	5.9818e-04	0.030	0.010	0.101	5.046

Figs. 12 to 15 demonstrate that the estimated values are in good agreement with experimental measurements. The fitting plot of training data for all the models shows the R-squared value close to 1. Meanwhile, experimental results also show that all models were able to estimate outputs with excellent accuracy of about 95%. The results confirm that the LSTM networks are well-suited to find relationships among features and can be used for making predictions based on time series data. One of the main reasons for LSTM networks' reasonable performance is the recurrent nature of this neural network and the presence of loops and gates within its iterative blocks, which allow past information to remain in the network and be used in decisions. Traditional recurrent neural networks cannot recall and use information from the distant past, so LSTM neural network with its new concepts was developed to overcome this weakness (Zhao et al., 2020).

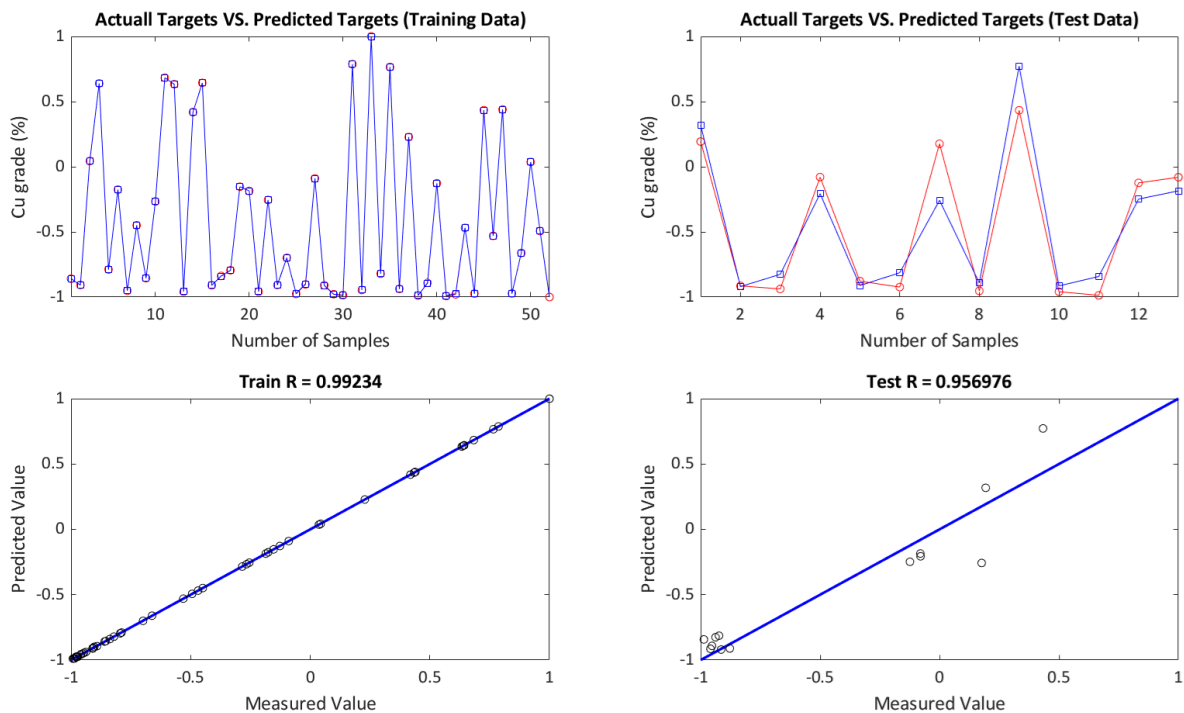


Fig. 12. Results of training and testing data for estimating Cu grade using LSTM network

Using the developed networks, the desired output could be estimated with a great accuracy. But another crucial point is to understand how much each input variables affect the desired output(s). Since neural networks are black boxes and studying their structure have not given us any insights on

the structure of the function being approximated, the importance and impact of each input variable on the output should be specified. As described by Pu et al. (2020), we can calculate the change of the model estimation error when an input value is randomly shuffled. If the model relies on an input for estimation, the model estimation error is expected to increase by permuting that input value. Because four models were developed for the outputs, the mentioned process was performed for all four models and the results of which are shown in Fig. 16. For instance, if the importance of features is determined in a processing plant, when changes in system output occur, if the gap between the output of the process and the desired output is wide, the more important inputs can be changed. If this gap is narrow, adjusting input values with low impact on outputs is recommended.

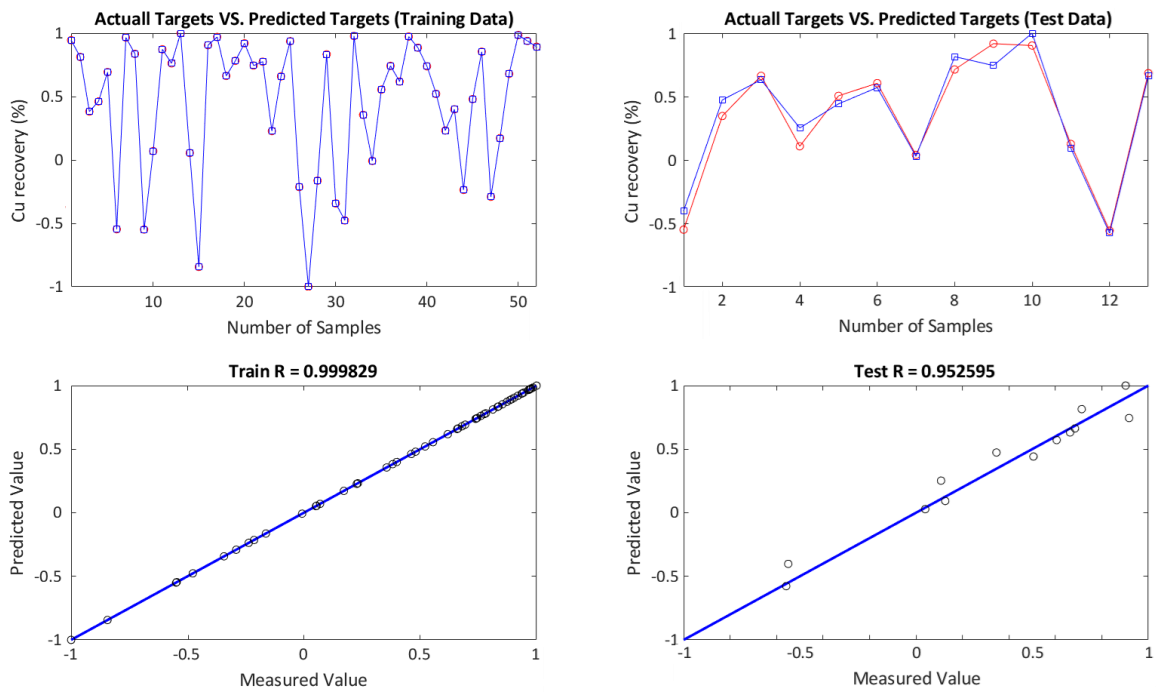


Fig. 13. Results of training and testing data for estimating Cu recovery using LSTM network

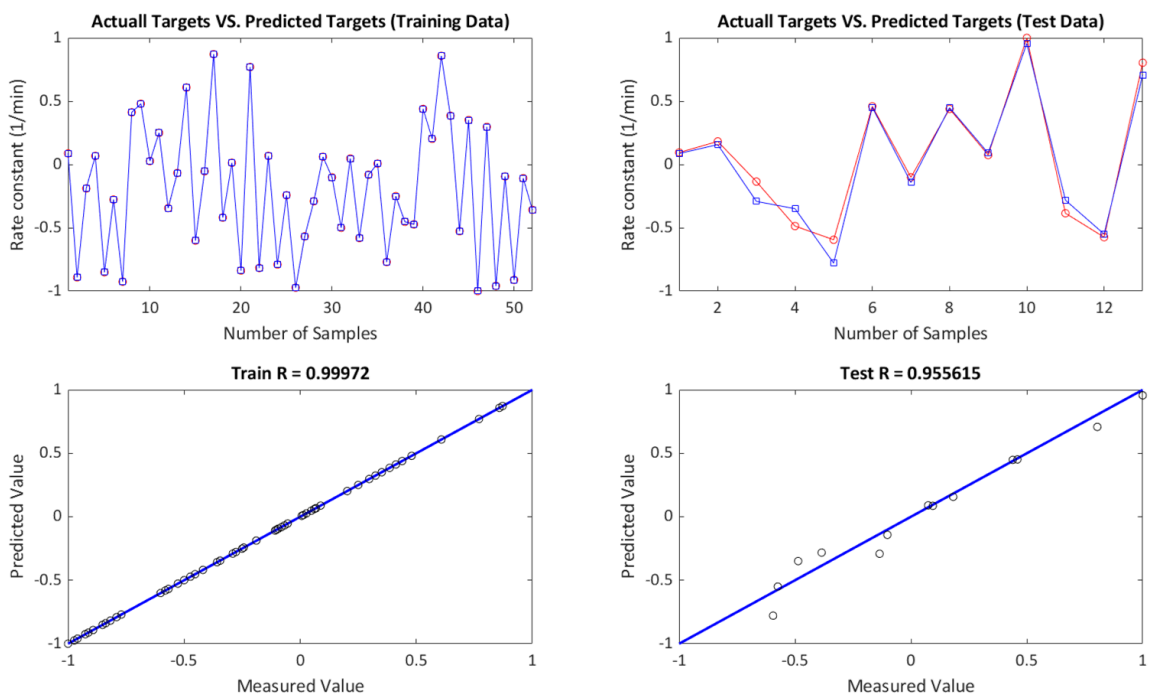


Fig. 14. Results of training and testing data for estimating Cu kinetics rate using LSTM network

It is noteworthy that the results of the features importance process are in good agreement with the ANOVA results (Tables A4 to A7), and the effects of mineralogical factors on outputs are more significant. In addition to accuracy, features importance results along with HD results, can also confirm that the LSTM method has been successful in developing models and extract meaningful characteristics from the training data. Despite the successful estimation of LSTM in this study, black-box property of LSTM or even all deep learning methods remains a challenge and requires further investigations. We expect to adjust desired output(s) by changing inputs based on features importance investigation but it cannot provide a quantitative relationship between inputs and outputs due to the lack of an explicit function. Thus, it is unknown how much of the alternation for each input value can result in the expected output values. So, as a suggestion for future research, quantifying the significance of input variables should be an issue for future works.

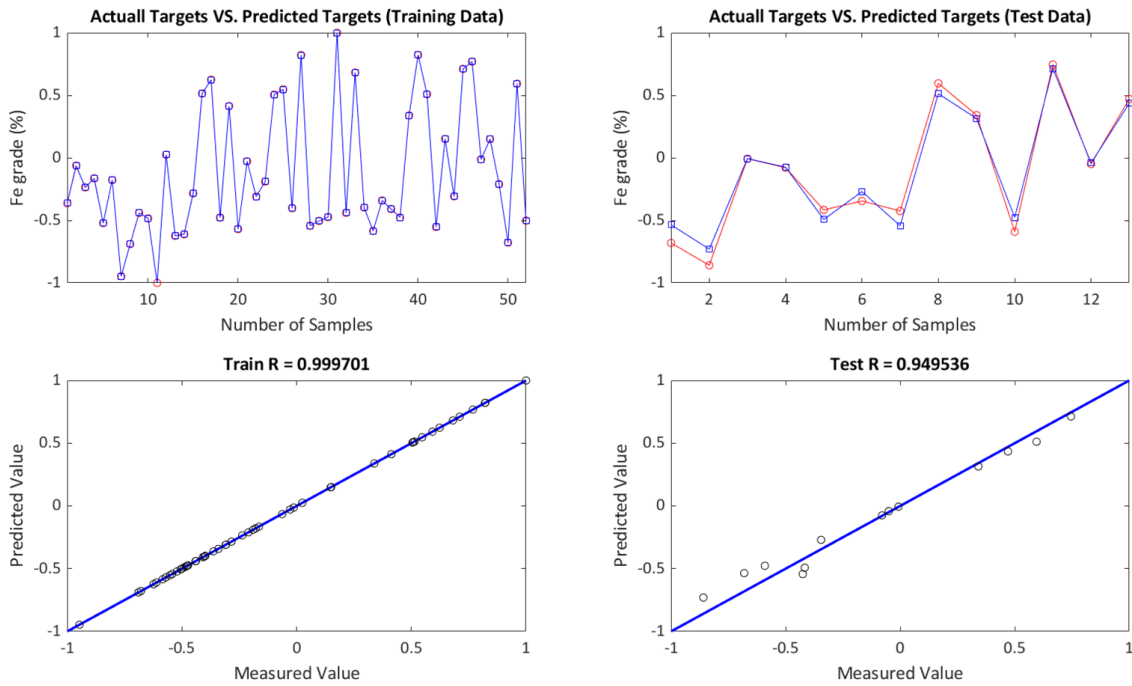


Fig. 15. Results of training and testing data for estimating Fe grade using LSTM network

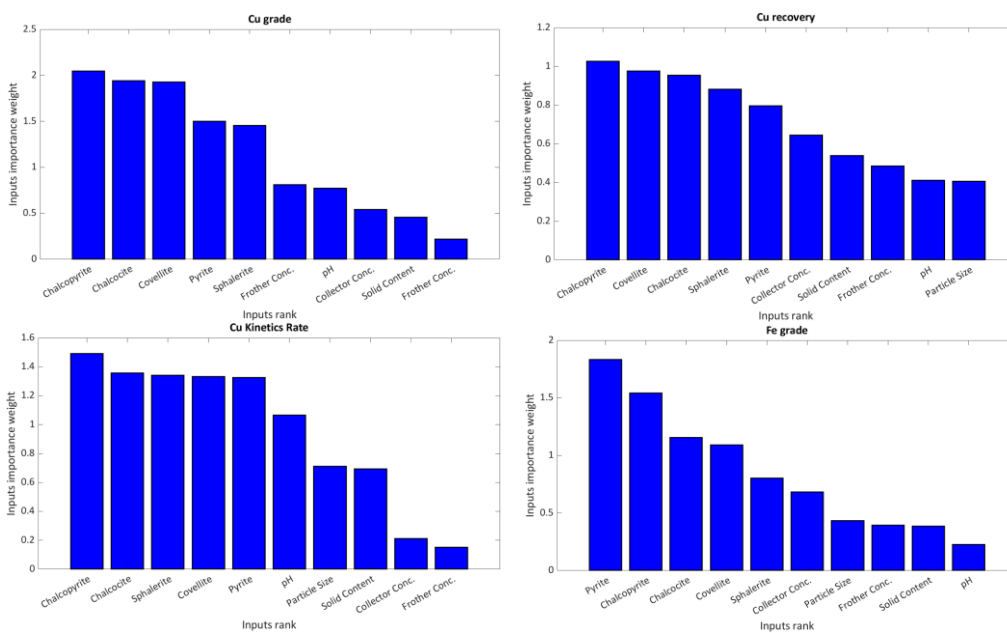


Fig. 16. Importance of features for process responses in the LSTM network

4. Conclusions

Despite the necessity of metallurgical studies in every mining activity to achieve sustainable production and products with optimal quality and quantity, the need for multiple test works, large volumes of sample characterization analyses, large amounts of data and, consequently, the need to spend considerable time and cost are significant challenges for such studies. The new approach of hybrid geometallurgy presented in this research is a solution by which the most important goal of geometallurgical studies i.e., to create a meaningful bridge between mining information and in particular mineralogical information, and metallurgical information in the mineral processing unit, can be vindicated using archived data and the efficient statistical method of historical data (HD) with minimal time and cost. Moreover, by simulating the refined results of HD studies using the deep learning (DL) method, an intelligent model can be developed to predict the operational responses of the mineral processing sector. The proposed structure for hybrid geometallurgical studies is schematically presented in Fig. 17.

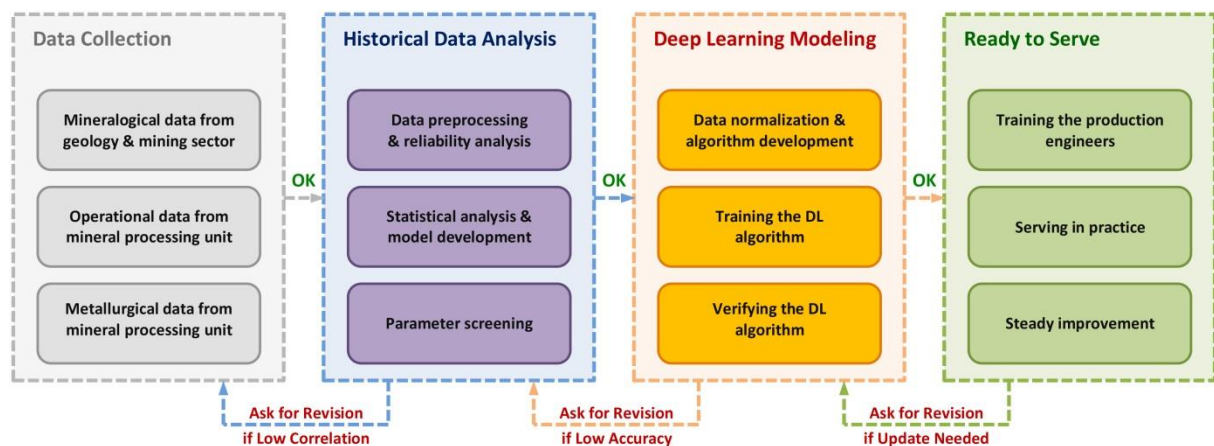


Fig. 17. Recommended main steps involved in hybrid geometallurgical studies

The efficiency of this proposed method was evaluated for a ore samples obtained from a copper mine. HD analyses revealed that the mineralogical and operational parameters can be correlated to the metallurgical responses with correlation coefficients around 90%. The significance of the studied factors was examined through ANOVA with Fisher and probability factors. Considering the significant parameters as inputs to the DL algorithm, simulation results showed that the process behaviour including the copper grade and recovery, copper kinetics constant and iron grade in concentrate in this study, could be predicted with more than 95% accuracy. In addition, one of the most important features of this approach is the possibility of considering a number of more effective parameters in the geometallurgical model. Future applications for the current geometallurgical approach may include the evaluation of exploration prospects, contributions to feasibility studies and providing assistance to optimise metallurgical processes. The Hybrid geometallurgical approach can also be useful to the other mineral industries as it is generically structured and can be modified to accommodate other ore types and different processing flow sheets.

References

- AGHELLI, A., HASSANZADEH, A., HASSAS, B.V., HASANZADEH, M., 2018. *Effect of pyrite content of feed and configuration of locked particles on rougher flotation of copper in low and high pyritic ore types*. Int. J. Min. Sci. Technol. 28(2), 167–176.
- ALRUIZ, O.M., MORRELL, S., SUAZO, C.J., NARANJO, A., 2009. *A novel approach to the geometallurgical modelling of the Collahuasi grinding circuit*. Miner. Eng. 22, 1060–1067.
- AMER, T.E., EL ASSAY, I.E., REZK, A.A., EL KAMMAR, A.M., EL MANAWI, A.W., ABU KHOZIEM, H.A., 2014. *Geometallurgy and processing of North Ras Mohamed poly-mineralized ore materials, South Sinai, Egypt*. Int. J. Miner. Process. 129, 12–21.

- APAYDIN, H., FEIZI, H., SATTARI, M.T., COLAK, M.S., SHAMSHIRBAND, S., CHAU, K., 2020. *Comparative analysis of recurrent neural network architectures for reservoir inflow forecasting*. *Water* 12(5), 1500.
- ASADI, E., ISAZADEH, M., SAMADIANFARD, S., RAMLI, M.F., MOSAVI, A., NABIPOUR, N., SHAMSHIRBAND, S., HAJNAL, E., CHAU, K., 2020. *Groundwater quality assessment for sustainable drinking and irrigation*. *Sustain.* 12(1), 177.
- AZIZI, A., HASSANZADEH, A., FADAEI, B., 2015. *Investigating the first-order flotation kinetics models for Sarcheshmeh copper sulfide ore*. *Int. J. Min. Sci. Technol.* 25(5), 849–854.
- BECKER, M.A., HARRIS, P.G., WIESE, J.G., BRADSHAW, D.J., 2009. *Mineralogical characterisation of naturally floatable gangue in Merensky Reef ore flotation*. *Int. J. Miner. Process.* 93, 246–255.
- BENGIO, Y., SIMARD, P., FRASCONI, P., 1994. *Learning long-term dependencies with gradient descent is difficult*. *IEEE Trans. Neur. Net.* 5(2), 157–166.
- BERNICO, M., 2018. *Deep learning quick reference: useful hacks for training and optimizing deep neural networks with TensorFlow and Keras*. Packt Publishing Ltd., New York, USA.
- BOVEIRI, R., SHOJAEI, V., KHOSHDAST, H., 2019. *Efficient cadmium removal from aqueous solutions using a sample coal waste activated by rhamnolipid biosurfactant*. *J. Environ. Manag.* 231, 1182–1192.
- CALIN, O., 2020. *Deep learning architectures*. Springer Nature, Cham, Switzerland.
- DEHAINE, Q., FILIPPOV, L.O., GLASS, H.J., ROLLINSON, G.K., 2019. *Rare-metal granites as a potential source of critical metals: A geometallurgical case study*. *Ore Geol. Rev.* 104, 384–402.
- DEHAINE, Q., TIJSELING, L.T., GLASS, H.J., TÖRMÄNEN, T., BUTCHER, A.R., 2021. *Geometallurgy of cobalt ores: A review*. *Miner. Eng.* 160, 106656.
- DEHAINE, Q., TIJSELING, L.T., ROLLINSON, G.K., BUXTON, M.W.N., GLASS, H.J., 2022. *Geometallurgical characterisation with portable FTIR: Application to sediment-hosted Cu-Co ores*. *Miner.* 12, 15.
- FARROKHPAY, S., FILIPPOV, L., FORNASIERO, D., 2021. *Flotation of fine particles: A review*. *Miner. Process. Ext. Metal. Rev.* 42(7), 473–483.
- GHOBADI, P., YAHYAEI, M., BANISI, S., 2011. *Optimization of the performance of flotation circuits using a genetic algorithm oriented by process-based rules*. *Int. J. Miner. Process.* 98(3–4), 174–181.
- GHOLAMI, A.R., KHOSHDAST, H., 2020. *Using artificial neural networks for the intelligent estimation of selectivity index and metallurgical responses of a sample coal bioflotation by rhamnolipid biosurfactants*. *Ener. Res. A: Rec. Util. Environ. Eff.*, doi: 10.1080/15567036.2020.1857477.
- GHOLAMI, A.R., KHOSHDAST, H., HASSANZADEH, A., 2021. *Using hybrid neural networks/genetic and artificial bee colony algorithms to simulate the bio-treatment of dye-polluted wastewater using rhamnolipid biosurfactants*. *J. Environ. Manag.* 299, 113666.
- GRAVES, A., 2012. *Long short-term memory*. In *Supervised sequence labelling with recurrent neural networks*. Springer, Berlin, Germany.
- HASSANZADEH, A., AZIZI, A., KOUACHI, S., KARIMI, M., CELIK, M.S., 2019. *Estimation of flotation rate constant and particle-bubble interactions considering key hydrodynamic parameters and their interrelations*. *Miner. Eng.* 141, 105836.
- HASSANZADEH, A., FIROUZI, M., ALBIJANIC, B., CELIK, M.S., 2018. *A review on determination of particle-bubble encounter using analytical, experimental and numerical methods*. *Miner. Eng.* 122, 296–311.
- HASSANZADEH, A., KARAKAŞ, F., 2017a. *Recovery improvement of coarse particles by stage addition of reagents in industrial copper flotation circuit*. *J. Dis. Sci. Technol.* 38(2), 309–316.
- HASSANZADEH, A., KARAKAŞ, F., 2017b. *The kinetics modeling of chalcopyrite and pyrite, and the contribution of particle size and sodium metabisulfite to the flotation of copper complex ores*. *Part. Sci. Technol.* 35(4), 455–461.
- HOAL, K., 2008. *Getting the geo into geomet*. *SEG Newsl.* 73(73), 11–15.
- HOAL, K.O., APPLEBY, S.K., STAMMER, J.G., PALMER, C., 2009. *SEM-based quantitative mineralogical analysis of peridotite, kimberlite and concentrate*. *Lithos* 112, 41–46.
- HOCHREITER, S., SCHMIDHUBER, J., 1997. *Long short-term memory*. *Neur. Comput.* 9(8), 1735–1780.
- HOSEINIAN, F.S., ABDOLLAHZADE, A., MOHAMADI, S.S., HASHEMZADEH, M., 2017. *Recovery prediction of copper oxide ore column leaching by hybrid neural genetic algorithm*. *Trans. Nonfer. Metal Soc. China* 27(3), 686–693.
- HOSEINIAN, F.S., REZAI, B., KOWSARI, E., SAFARI, M., 2020. *A hybrid neural network/genetic algorithm to predict Zn (II) removal by ion flotation*. *Sep. Sci. Technol.* 55(6), 1197–1206.

- JORJANI, E., BAGHERIEH, A., MESROGHLI, S., CHELGANI, S.C., 2008. *Prediction of yttrium, lanthanum, cerium, and neodymium leaching recovery from apatite concentrate using artificial neural networks*. J. Uni. Sci. Technol. Beijing Miner Metal. Mater. 15(4), 367–374.
- KHOSHDAST, H., GHOLAMI, A.R., HASSANZADEH, A., NIEDOBA, T., SUROWIAK, A., 2021. *Advanced simulation of removing chromium from a synthetic wastewater by rhamnolipidic bioflotation using hybrid neural networks with metaheuristic algorithms*. Mater. 14, 2880.
- KHOSHDAST, H., SAM, A., MANAFI, Z., 2012. *The use of rhamnolipid biosurfactants as a frothing agent and a sample copper ore response*. Miner. Eng. 26, 41–49.
- KHOSHDAST, H., SAM, A., VALI, H., AKBARI NOGHABI, K., 2011. *Effect of rhamnolipid biosurfactants on performance of coal and minerals flotation*. Int. Biodeter. Biodegrad. 65, 1238–1243.
- LANG, A.M., AASLY, K., ELLEFMO, S.L., 2018. *Mineral characterization as a tool in the implementation of geometallurgy into industrial mineral mining*. Miner. Eng. 116, 114–122.
- LE, X.H., HO, H.V., LEE, G., JUNG, S., 2019. *Application of long short-term memory (LSTM) neural network for flood forecasting*. Water 11(7), 1387.
- LUND, C., LAMBERG, P., LINDBERG, T., 2013. *Practical way to quantify minerals from chemical assays at Malmberget iron ore operations – An important tool for the geometallurgical program*. Miner. Eng. 49, 7–16.
- MILIVOJEVIC, M., STOPIC, S., FRIEDRICH, B., STOJANOVIC, B., DRNDAREVIC, D., 2012. *Computer modeling of high-pressure leaching process of nickel laterite by design of experiments and neural networks*. Int. J. Miner. Metal. Mater. 19(7), 584–594.
- MONTGOMERY, D.C., 2001. *Design and analysis of experiments*. John Wiley & Sons, New York, USA.
- NAVARRA, A., MENZIES, A., JORDENS, A., WATERS, K., 2017. *Strategic evaluation of concentrator operational modes under geological uncertainty*. Int. J. Miner. Process. 164, 45–55.
- PARIAN, M., LAMBERG, P., MÖCKEL, R., ROSENKRANZ, J., 2015. *Analysis of mineral grades for geometallurgy: Combined element-to-mineral conversion and quantitative X-ray diffraction*. Miner. Eng. 82, 25–35.
- PARIAN, M., LAMBERG, P., ROSENKRANZ, J., 2018a. *Process simulations in mineralogy-based geometallurgy of iron ores*. Miner. Proc. Ext. Metal., doi: 10.1080/25726641.2018.1507072.
- PARIAN, M., MWANGA, A., LAMBERG, P., ROSENKRANZ, J., 2018b. *Ore texture breakage characterization and fragmentation into multiphase particles*. Powder Technol. 327, 57–69.
- PÉREZ-BARNUEVO, L., LÉVESQUE, S., BAZIN, C., 2018. *Drill core texture as geometallurgical indicator for the Mont-Wright iron ore deposit (Quebec, Canada)*. Miner. Eng. 122, 130–141.
- PHILANDER, C., ROZENDAAL, A., 2013. *The application of a novel geometallurgical template model to characterise the Namakwa Sands heavy mineral deposit, West Coast of South Africa*. Miner. Eng. 52, 82–94.
- PHILANDER, C., ROZENDAAL, A., 2014. *A process mineralogy approach to geometallurgical model refinement for the Namakwa Sands heavy minerals operations, west coast of South Africa*. Miner. Eng. 65, 9–16.
- PU, Y., SZMIGIEL, A., APEL, D.B., 2020. *Purities prediction in a manufacturing froth flotation plant: the deep learning techniques*. Neur. Comput. App., 1–11.
- SCHÖBER, P., BOER, C., SCHWARTE, L.A., 2018. *Correlation coefficients: appropriate use and interpretation*. Anes. Anal. 126(5), 1763–1768.
- SHAK, K.P.Y., WU, T.Y., 2015. *Optimized use of alum together with unmodified Cassia obtusifolia seed gum as a coagulant aid in treatment of palm oil mill effluent under natural pH of wastewater*. Ind. Crop. Prod. 76, 1169–1178.
- SHAMSHIRBAND, S., HASHEMI, S., SALIMI, H., SAMADIANFARD, S., ASADI, E., SHADKANI, S., KARGAR, K., MOSAVI, A., NABIPOUR, N., CHAU, K., 2020. *Predicting standardized streamflow index for hydrological drought using machine learning models*. Eng. App. Comput. Fluid Mech. 14(1), 339–350.
- SOBOUTI, A., HOSEINIAN, F.S., REZAI, B., JALILI, S., 2019. *The lead recovery prediction from lead concentrate by an artificial neural network and particle swarm optimization*. Geosys. Eng. 22(6), 319–327.
- TRIFFETT, B., VELOO, C., ADAIR, B.J.I., BRADSHAW, D., 2008. *An investigation of the factors affecting the recovery of molybdenite in the Kennecott Utah copper bulk flotation circuit*. Miner. Eng. 21, 832–840.
- TUNGPALAN, K., MANLAPIG, E., ANDRUSIEWICZ, M., KEENEY, L., WIGHTMAN, E., EDRAKI, M., 2015. *An integrated approach of predicting metallurgical performance relating to variability in deposit characteristics*. Miner. Eng. 71, 49–54.
- UZAIR, M., JAMIL, N., 2020. *Effects of hidden layers on the efficiency of neural networks*. In: 2020 IEEE 23rd International Multitopic Conference (INMIC), November, p.p. 1–6.

- VYAS, S., DAS, S., TING, Y-P., 2020. *Predictive modeling and response analysis of spent catalyst bioleaching using artificial neural network*. *Biores. Technol. Rep.* 9, 100389.
- YETILMEZSOY, K., DEMIREL, S., VANDERBEL, R.J., 2009. *Response surface modeling of Pb(II) removal from aqueous solution by Pistacia vera L.: Box-Behnken experimental design*. *J. Hazard. Mater.* 171, 551–562.
- YINGLING, J., 1990. *Circuit analysis: optimizing mineral processing flowsheet layouts and steady-state control specifications*. *Int. J. Min. Process.* 29, 149–174.
- ZHAO, J., HUANG, F., LV, J., DUAN, Y., QIN, Z., LI, G., TIAN, G., 2020. *Do RNN and LSTM have long memory?*. In: *International Conference on Machine Learning*, November, pp. 11365–11375.

APPENDIX

Table A1. The statistical summary of the data used in simulation process

Type of variable	Variable	Minimum	Mean value	Maximum	Standard deviation
Operating conditions	Particle size (μm)	63	103.909	110	14.253
	Collector concentration (g/t)	32	36.818	40	1.762
	Frother concentration (g/t)	10	13	16	1.289
	Solid content (%w/w)	25	30	35	2.148
Mineralogical data	pH	11	11.500	12	0.215
	Chalcocite (%)	0.021	0.115	0.330	0.102
	Covellite (%)	0.004	0.038	0.077	0.029
	Chalcopyrite (%)	0.058	0.876	2.454	0.889
	Pyrite (%)	5.334	8.793	17.196	4.529
	Sphalerite (%)	0.109	0.167	0.274	0.053
	Cu grade (%)	1.050	7.493	23.490	6.730
Operating responses	Cu recovery (%)	14.100	72.677	96.220	21.453
	Fe grade (%)	0.110	1.390	3.070	0.758
	Cu kinetics rate (1/min)	7.010	19.595	35.500	7.221

Table A2. Results of Kolmogorov-Smirnov test of normality

	Mean	Std. deviation	Absolute	Positive	Negative	Test Statistic	two-tailed <i>p</i> -value
Particle size	103.910	14.253	0.484	0.335	-0.484	0.484	0.000
Collector conc.	36.820	1.762	0.450	0.368	-0.450	0.450	0.000
Frother conc.	13.000	1.289	0.409	0.409	-0.409	0.409	0.000
Solid content	30.000	2.148	0.409	0.409	-0.409	0.409	0.000
pH	11.500	0.215	0.409	0.409	-0.409	0.409	0.000
Chalcocite	0.115	0.102	0.367	0.367	-0.178	0.367	0.000
Covellite	0.038	0.029	0.272	0.272	-0.242	0.272	0.000
Chalcopyrite	0.876	0.885	0.305	0.305	-0.178	0.305	0.000
Pyrite	8.793	4.529	0.352	0.352	-0.222	0.352	0.000
Sphalerite	0.167	0.053	0.307	0.307	-0.144	0.307	0.000
Cu grade	7.493	6.731	0.227	0.227	-0.169	0.227	0.000
Cu recovery	72.677	21.453	0.172	0.136	-0.172	0.172	0.000
Rate constant	1.390	0.758	0.059	0.059	-0.051	0.059	0.200
Fe grade	19.595	7.221	0.135	0.135	-0.104	0.135	0.005

Table A3. Parameter values of long short-term memory neural network

Parameters	Value
Batch size	10
Max epochs	40
Gradient threshold	0.500
Initial learn rate	0.005
Learn rate drop period	7
Learn rate drop factor	0.200

Table A4. Analysis of variance results for copper grade as process response

Source	Sum of squares	df	Mean square	F-value	<i>p</i> -value (Prob > F)
Particle size (d_{80})	18.5138	1	18.5138	4.34528	0.0421
Collector conc. (C)	12.3419	1	12.3419	8.96694	0.0095
Frother conc. (F)	28.2270	1	28.2270	6.62501	0.0042
Solid content (X)	13.7593	1	13.7593	3.22937	0.0078
pH	42.5164	1	42.5164	9.97881	0.0032
Chalcocite (Cc)	161.8362	1	161.8362	37.9837	< 0.0001
Covellite (Co)	79.61797	1	79.61797	18.6867	< 0.0001
Chalcopyrite (Cp)	375.3417	1	375.3417	88.0945	< 0.0001
Pyrite (Py)	217.0748	1	217.0748	50.9485	< 0.0001
Sphalerite (Sp)	205.7975	1	205.7975	48.3016	< 0.0001
Residual	217.2943	51	4.260673		
Cor total	2899.918	61			

Table A5. Analysis of variance results for copper recovery as process response

Source	Sum of squares	df	Mean square	F-value	<i>p</i> -value (Prob > F)
Particle size (d_{80})	1544.334	1	1544.334	3.8946	0.0541
Collector conc. (C)	439.0707	1	439.0707	11.0728	0.0298
Frother conc. (F)	1106.797	1	1106.797	27.9119	0.0101
Solid content (X)	233.149	1	233.149	5.8797	0.0447
pH	1646.409	1	1646.409	4.1520	0.0470
Chalcocite (Cc)	87886.13	1	87886.13	221.6372	< 0.0001
Covellite (Co)	52202.67	1	52202.67	131.6482	< 0.0001
Chalcopyrite (Cp)	56385.51	1	56385.51	142.1968	< 0.0001
Pyrite (Py)	37593.33	1	37593.33	94.8054	< 0.0001
Sphalerite (Sp)	43318.23	1	43318.23	109.2428	< 0.0001
Residual	19430.05	49	396.5316		
Cor total	335682.6	59			

Table A6. Analysis of variance results for iron grade as process response

Source	Sum of squares	df	Mean square	F-Value	<i>p</i> -value (Prob > F)
Particle size (d_{80})	740.4	1	740.4	12.62	0.0008
Collector conc. (C)	23.67	1	23.67	4.00	0.0053
Frother conc. (F)	6.02	1	6.02	1.00	0.0075
Solid content (X)	10.95	1	10.95	1.90	0.0067
pH	312.12	1	312.12	5.32	0.025
Chalcocite (Cc)	4355.44	1	4355.44	74.24	< 0.0001
Covellite (Co)	2623.98	1	2623.98	44.73	< 0.0001
Chalcopyrite (Cp)	3238.89	1	3238.89	55.21	< 0.0001
Pyrite (Py)	2602.31	1	2602.31	44.36	< 0.0001
Sphalerite (Sp)	2287.92	1	2287.92	39	< 0.0001
Residual	3109.29	53	58.67		
Cor total	26465.92	63			

Table A7. Analysis of variance results for kinetics rate as process response

Source	Sum of squares	df	Mean square	F-value	<i>p</i> -value (Prob > F)
Particle size (d_{80})	2.5839	1	2.5839	7.5469	0.0082
Collector conc. (C)	1.4637	1	1.4637	4.2753	0.0436
Frother conc. (F)	5.0389	1	5.0389	14.7174	0.0230
Solid content (X)	8.5330	1	8.5330	2.4924	0.0087
pH	4.0242	1	4.0242	11.75393	0.0012
Chalcocite (Cc)	28.921	1	28.921	84.47173	< 0.0001
Covellite (Co)	23.8472	1	23.8472	69.65239	< 0.0001
Chalcopyrite (Cp)	16.5967	1	16.5967	48.47531	< 0.0001
Pyrite (Py)	8.8358	1	8.8358	25.80754	< 0.0001
Sphalerite (Sp)	7.7142	1	7.7142	22.53156	< 0.0001
Residual	18.1459	53	0.3424		
Cor total	155.2911	63			